超過外力に対する河川堤防の耐水性能評価と流域減災システムへの適用に関する研究

AUTHOR(S):

東, 良慶; 関口, 秀雄; 小野, 徹

CITATION:

東, 良慶 ...[et al]. 超過外力に対する河川堤防の耐水性能評価と流域減災システムへの適用に関する研究. 京都大学防災研究所年報. C 2006, 49(C): 225-235

ISSUE DATE:

2006-04-01

URL:

http://hdl.handle.net/2433/26691

京都大学防災研究所年報 第 49 号 C 平成 18 年 4 月
Annuals of Disas. Prev. Res. Inst., Kyoto Univ., No. 49 C, 2006

Performance of Levee System at Flood Stage

Ryoukei AZUMA, Hideo SEKIGUCHI and Tetsu ONO*

*Dept. of Urban and Environment Engineering, Kyoto University

Synopsis

This study was motivated by the October 2004 levee-breaching case in the Maruyama River that took place under extremely high flood stage. The overflow and outburst brought about a range of sedimentary features to an adjacent paddy field with clayey subsoil. They included a plunge pool and two massive particulate ridges which were formed on either side of the central erosion-dominant zone. The breaching-induced topographical changes were precisely measured using digital photogrammetry and incorporated into a geographical information system (GIS), facilitating an analysis of the sediment budget. The severity of the inundating water was assessed based on a bedload transport theory, with the observation that only the large clay lumps were left on the central erosion-dominant zone. Furthermore, a discussion is made of the usefulness and limitations in a specially designed yet print-based, geomorphological classification map for the flood-prone Maruyama River basin that has witnessed land-use evolution over the past thirty years since its initial publication.

Keywords: Crevasse splay sediment, Levee breaching, Digital photo-theodolite survey

1. Introduction

The urbanization in river basins and increased trend of extreme meteorological events have recently intensified flood disasters in Japan. Admittedly, however, it is unrealistic to make every river reach sided by high levees in such a way that no overflow can occur even under excessively high flood stage.

The question then arises as to how the consequences of such flooding may be minimized. One of the possible ways along that line may be to strengthen levees in a form resilient enough to withstand overflowing water, thereby providing lead time for early warning and evacuation. Another, equally important strategy will focus on careful land-use planning for flood-prone river basins. Up to now, the outcome of such an approach has been published in the form of geomorphological classification map for flooding-vulnerable areas (e.g., Oya *et al*., 1998). It is a pleasing observation that the Geographical Survey Institute (GSI) has recently taken initiatives in publishing such specially designed, geomorphological classification maps for major river basins which remained out of print for a long time. We consider that they will become even more effective and flexible if represented in a digital format so as to enable regular updating in view of land-use evolution and other such important factors.

With the above-mentioned in mind, this study attempts to promote an insight into crevasse-splay sedimentation. Salient knowledge of this may be useful for engineered levee construction in flood-stricken areas. Specifically, this study was motivated by a levee -breaching case with the Maruyama River that took place in association with typhoon 0423. We noted that the flood-induced overflow and outburst brought about a range of distinct sedimentary features to the adjacent paddy field.

In what follows, we will first outline the flood disaster induced by typhoon 0423. This is followed by a description of the digital photo-theodolite system which

we used for precise measurements of the breaching -induced topographical changes. The results obtained will then be worked out, facilitating a sediment budget analysis. Then, flow-out velocities over the flood plain will be estimated in light of a bedload transport theory. Moreover, practical implications of a geographical classification map for the flood-stricken Maruyama River basin will be pointed out, with future direction of extension.

2. The October 2004 flood disaster in Maruyama River basin

The Maruyama River runs through a northern part of Hyogo Prefecture via the low-lying Toyooka Basin and drains into Japan Sea (Fig. 1). Typhoon 0423 made landfall in Osaka at 18:00 on 20 October 2004. It brought about precipitation as much as 278mm in the Toyooka area over a two-day period (20-21 October 2004). The associated hydrograph obtained at the Tachino Observatory (Toyooka Office, 2005a) is shown in Fig. 2. It is seen that the water level started rising from around 14:00 on October 20 and rapidly increased thereafter, exceeding the design high-water level (T.P. +8.16m) at around 21:00. Eventually, the maximum water level rose as high as T.P. +8.29m.

According to testimony of residents, the overflow occurred at Tachino around 21:00 on 20 October 2004 on the right bank of the Maruyama River. Approximately two hours later, the right bank breached, bringing about serious damage to the adjacent buildings, facilities and paddy field.

3. Digital photo-theodolite survey

3.1 Aims of the digital photogrammetry

Visits to the breaching-affected area made us notice a range of marked sedimentary features such as shown in Photo. 1 (Azuma *et al*., 2005). In this photograph one may note the central water body (erosional feature) and two distinct piles of particulate matter (depositional feature; ridges 1 and 2). In order to precisely evaluate these and other related topographical changes, we selected and used the method of digital photo-theodolite surveying (Ono and Hattori, 2002; Ono *et al*., 2004). The features of the method will be described below.

Fig. 1 A map showing the Maruyama River course

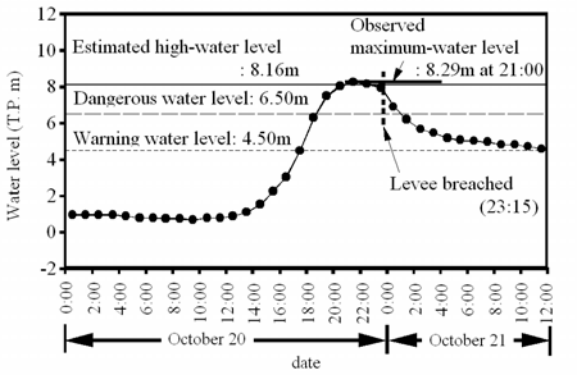

Fig. 2 Hydrograph obtained at Tachino observatory on October 20-21 (adapted from Toyooka office, 2005a)

3.2 Features of the digital photo-theodolite survey

The digital photo-theodolite method is a "non-invasive" one. This feature was crucial for field survey in view of the fact that the paddy field is individuals' property. We selected only four positions of photographing on the crown of the provisionally rebuilt section of the levee (Fig. 3). The hardware used consisted of a digital camera that was mounted on a theodolite (Fig. 4). The digital camera had eight megapixels, allowing a high spatial resolution. The theodolite facilitated the measurement of two angles of orientation on vertical and horizontal planes at every photographing position.

Photo. 1 Panoramic view showing consequences of levee breaching at Tachino, as of December 22, 2004

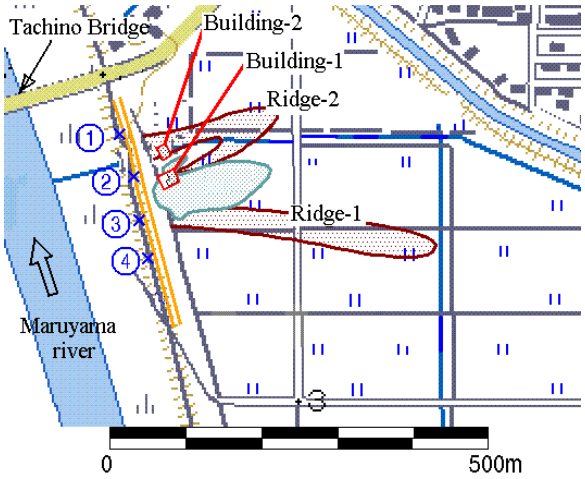

Fig. 3 Camera positions in digital photogrammetry

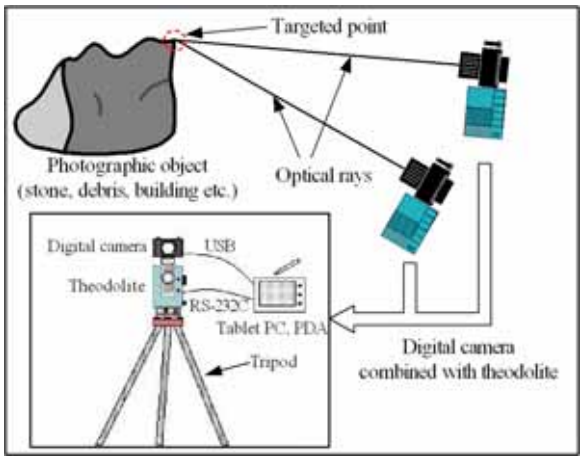

Fig. 4 Digital photo-theodolite system, together with identification method of an object

The three-dimensional coordinates of a targeted object may be determined based on the method of spatial intersection. In essence, a pair of two photographs of the targeted point from two different positions permits its three-dimensional coordinates to be determined.

3.3 Evaluation of breaching-induced topographical changes in flood plain

A total of 1029 points were identified in the affected flood plain using the photo-theodolite method. Technically, a key for the identification was to seek objects that had sharp corners. For this purpose, angular stones or debris made a good target. The locations of those identified points are projected onto a horizontal plane and are represented using an *x-y* coordinate system, with the camera position No.3 being chosen as the origin (Fig. 5). Note herein that the reference horizontal plane was selected at a level numerically equal to the surface of the water body at the time of photographing.

The relative heights of the identified survey points are shown in Fig. 6 in terms of contours. These contours were constructed using ArcGIS software (ESRI). It is noted that ridge-1 extended 300 meters in a direction

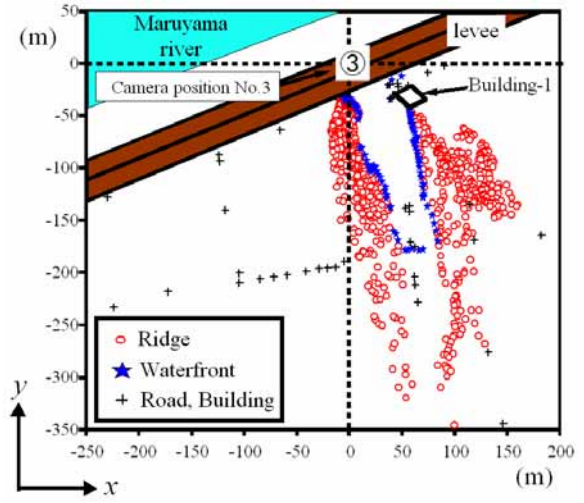

Fig. 5 Identified survey points plotted on the *x-y* coordinate system indicated

nearly normal to the levee. The height of the ridge took a maximum value (2.2m) near the levee and decreased gradually with distance from the levee. The occurrence of ridge-2 is also apparent in Fig. 6. A close look at Fig. 6 suggests the presence of another, much shallower pile of sediment (ridge-3) at the far end of the central erosional region where most of the outbursts were

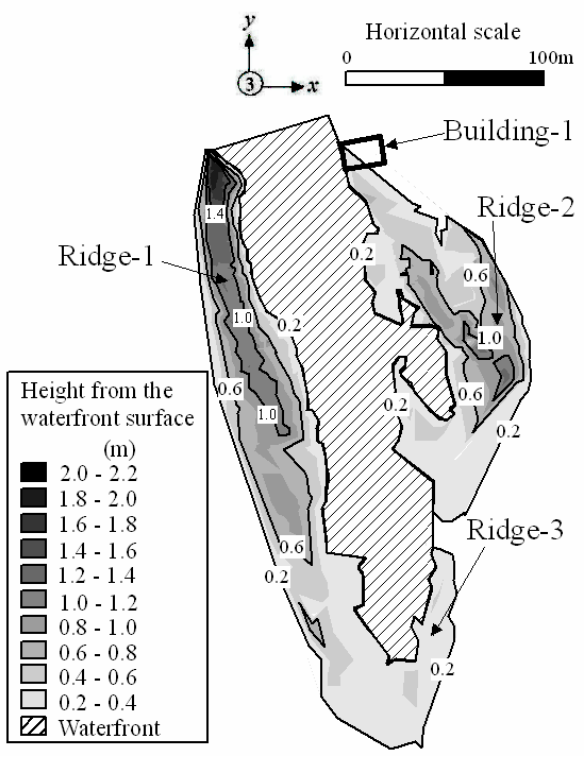

Fig. 6 Contours showing topographical changes induced in the flood plain

believed to flow down.

An aerial photograph of the affected flood plain is shown in Photo. 2 (courtesy of Prof. Y. Fujita). In this photograph, ridges 1, 2 and 3 are clearly visible. The extents of ridges 1 and 2 appear to be in general conformity with the contour plots shown in Fig. 6. Although Rigde-3 manifests itself as a relatively narrow strip of sediment in Photo. 2, it is only marginally discernible in Fig. 6. This performance suggests that ridge-3 was a less pronounced feature and was likely to have undergone secondary modifications.

4. Sediment volume analysis

4.1 Volumes of ridge-1 and ridge-2

In order to evaluate the volume of deposition of ridge-1, we covered the ridge with a computational grid of 100 rows by 11 columns (Fig. 7). The grid intervals were set at 3.0m. The use of ArcGIS permitted us to evaluate the cross-sectional area of the ridge along each grid line. Thus the volume of ridge-1 was evaluated to be 12000 m^3. In the course of the volume analysis for ridge-1, we obtained the surface profile along each grid line. Those results are integrated to give a three-dimensional representation such as shown in Fig. 8.

Ridge-2 took a horseshoe shape behind Building-1 and Building -2 as shown in Photo. 2. The maximum height of ridge-2 was 1.4m and appeared near the levee. The volume of ridge-2 was evaluated to be equal to 5000m^3.

4.2 Volume of breached levee section

A plan view of the breached levee section approximately 100 m wide is presented in Fig. 9. In order to calculate the volume of loss due to the breaching, we chose a section marked A-A' on Fig. 9, which was located 80m upstream from the breached section. The cross-section through A-A' is shown in Fig. 10. Note in this figure that the body of soil above the dotted line represents the volume of the levee material lost due to the breaching. Note herein that we drew the dividing line

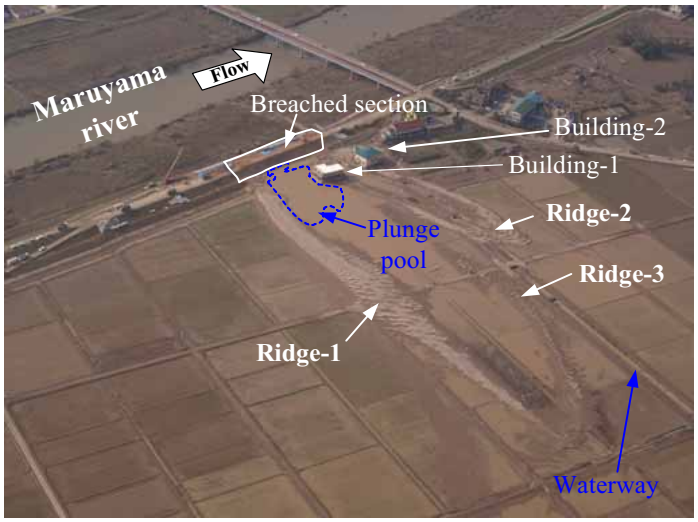

Photo. 2 Aerial photograph of the flood plain, taken on October 25, 2004 (courtesy of Prof. Y. Fujita)

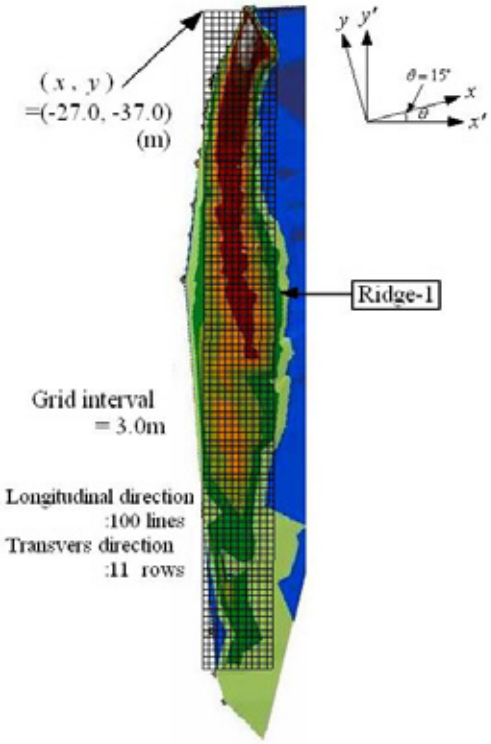

Fig. 7 Computational grid covering ridge-1

in such a way as to pass through the riverside toe of the levee (T.P.+4.3m) and to meet with the edge of the plunge pool (T.P.+1.16m). The calculation of the volume above the dotted line was then straightforward. Namely, the area multiplied by the 100m length gave rise to the volume of loss of the levee equal to 16000m^3.

4.3 Volume of plunge pool

Let us first look at Photo. 3 that captures the sedimentary features of the plunge pool and adjacent areas. The periphery of the plunge pool had nearly vertical faces. This feature is compatible with the observation that the plunge pool was formed by scouring of the clayey subsoil in the paddy field. Also, a close look at Photo. 3 beyond the plunge pool shows the

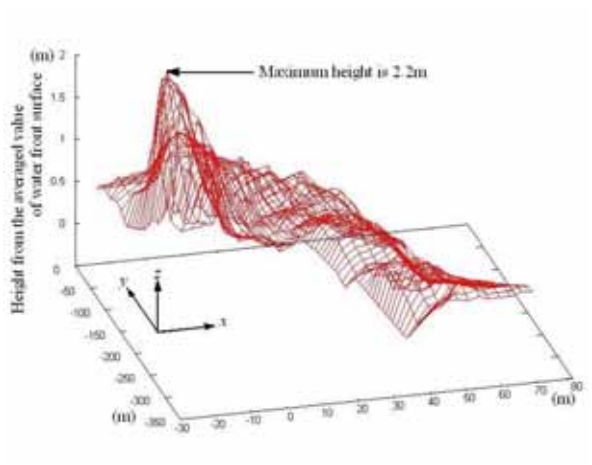

Fig. 8 The surface topography of ridge-1 by three-dimensional representation

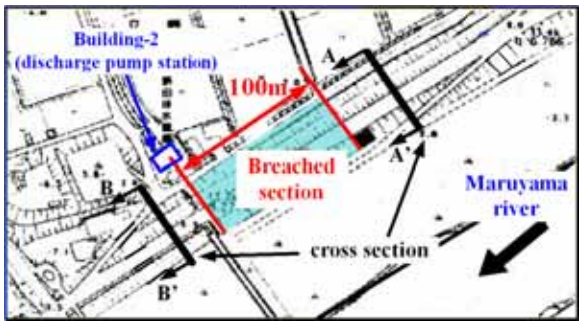

Fig. 9 Map showing the extent of the breached section

presence of a number of clay lumps that were produced by scouring, transported and finally left on the affected flood plain. The size of the clay lumps has a practical implication and will be referred to later in this paper.

Let us now focus the discussion on the configuration of the plunge pool (Toyooka Office, 2005a). The plunge pool was 54m long and 45m wide in plan (Fig. 11). Its maximum depth was 4.3m from the ground surface, whose average elevation was T.P.+1.16m. In order to evaluate the volume of the plunge pool, we simplified the configuration as shown in Fig. 12. Then the volume

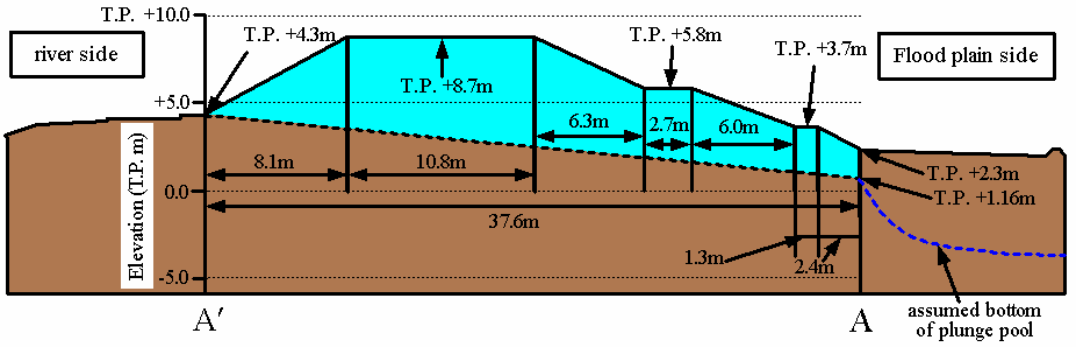

Fig. 10 Cross-section A-A' through the levee (Toyooka office, 2005a). We have added the dividing bottom line.

Photo. 3 A view of plunge pool and adjacent areas (photograph taken on November 25, 2004)

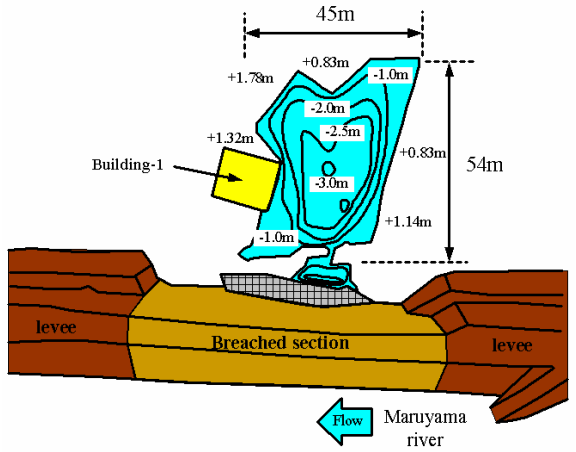

Fig. 11 Contours of equal elevations, in terms of T.P., of the plunge pool and surrounding ground surface (adapted from Toyooka office, 2005a)

of the plunge pool, V, was calculated as

$$V = A_1h_1 + A_2h_2 + A_3h_3 + A_4h_4 + A_5h_5 \quad (1)$$

where A_i represents the area of the horizontal cross-section designated and h_i stands for the thickness between the two horizontal planes involved. Thus the volume of the plunge pool was estimated to be equal to 5000m^3.

4.4 Comparison of volumes of erosion and deposition in associated with levee breaching

The volumes of erosion and deposition that are estimated in the previous sub-sections are summarized in Table 1. The volume of transfer by erosion is equal to 21000m^3 which is the sum of the 16000m^3 from the breached levee and the 5000m^3 from the plunge pool. The volume of deposition is equal to 17000m^3 which is

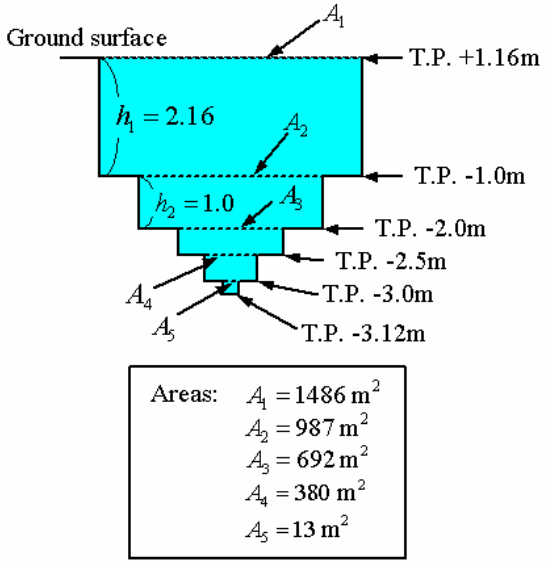

Fig. 12 Simplified representation of the configuration of the plunge pool

the sum of the 12000m^3 from ridge-1 and the 5000m^3 from ridge-2. It can then be concluded that the sediment yield due to the breaching largely resulted in the formation of ridges 1 and 2.

Table 1 Results of volume analysis

Sedimentary feature	Volume evaluated (m^3)
Breached levee	16000
Plunge pool	5000
Ridge-1	12000
Ridge-2	5000

5. Estimation of flow-out velocity in flood plain

As mentioned earlier, we noted the presence of a number of clay lumps in the flood plain beyond the plunge pool (Photo. 4). The clay lumps were evidently outsized, compared with the deposited sandy materials. The size of the large clay lumps were 50cm or so in diameter (Azuma *et al*., 2005). The question now arises as to how such clay lumps were formed. Our idea about this is schematically shown in Fig. 13. The stream power due to the overflow may be the principal agent for scouring the clayey subsoil in the paddy field, producing clay lumps. Indeed, if the clayey soil had a significant tensile strength, it could then fail in the form of blocks under the action of water jet or stream power; this failure mode should be contrasting with that of cohesionless sandy sediments.

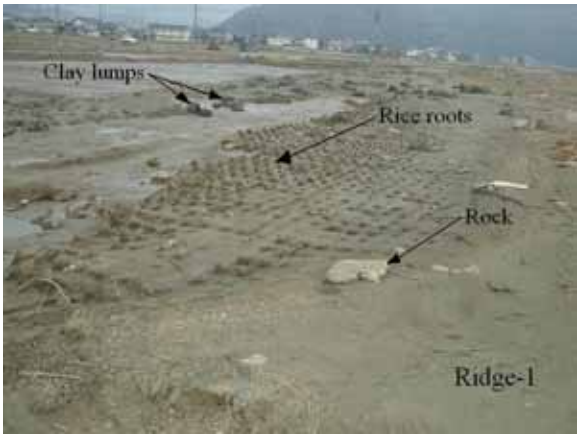

Photo. 4 Clay lumps left on the severely eroded surface in the clayey subsoil

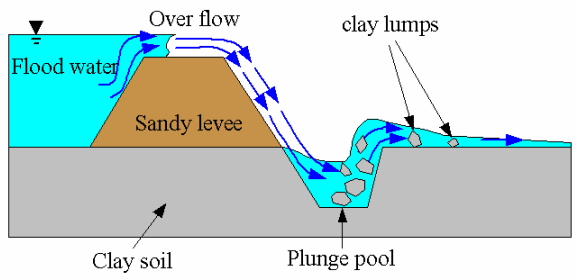

Fig. 13 Sketch illustrating the process of producing clay lumps

The Soil strata in cross sections A-A' and B-B' through the levee is shown in Fig. 14 where the assumed bottom line of plunge pool were added. It is noted that the clayey subsoil existed below the breached levee. As the plunge pool was formed, the clayey subsoil was scoured to form the clay lumps. Also, it is important in Fig. 14 to note that the seepage flow through the foundation soil was insignificant, if any, during the flood stage because of the sheet pile already provisioned.

Let us now make an attempt for estimating the intensity of the flow-out water. For this purpose, we assume that the transport of sediment debris, including clay lumps, occurs in the bedload regime. Let τ_{*c} be the intensity of the critical traction for incipient motion of a sediment particle, which is defined as

$$\tau_{*c} = \frac{u_{*c}^{\ 2}}{\{(\rho_s - \rho_f)/\rho_f\} \cdot g \cdot d} \tag{2}$$

where u_* = critical friction velocity, ρ_s = mass density of sediment; ρ_f = mass density of water; g = acceleration due to gravity and d = diameter of sediment. The critical friction velocity u_{*c} may be related to a representative velocity V_{0c} in the following form Uda *et al.*(1997) :

$$u_{*c} = V_{0c}/\phi \tag{3}$$

$$\phi = \left(\frac{1}{n}\right) \cdot \left(\frac{h^{1/6}}{\sqrt{g}}\right) \tag{4}$$

where ϕ = velocity coefficient, n = Manning's roughness coefficient, h = water depth. It follows from Eqs.(2) through (4) that

$$V_{0c} = \left(\tau_{*c} \cdot \frac{(\rho_s - \rho_f)}{\rho_f} \cdot d\right)^{1/2} \cdot \left(\frac{1}{n}\right) \cdot h^{\frac{1}{6}} \tag{5}$$

Equation (5) may be interpreted as being the equation that represents the functional dependence of the critical velocity V_{0c} upon the grain size, *d*. In order for this interpretation to work, we first note that

$$\tau_{*c} \cong 0.05 \tag{6}$$

for relatively large grain sizes (Iwagaki, 1956). The mass density of sediment is considered herein to range from ρ_s=1.9 to 2.7 g/cm^3. Note that a clay lump is a nearly saturated porous soil and thus has a relatively low, apparent density (say, ρ_s =1.9 g/cm^3). Manning's roughness coefficient, *n*, is a parameter that, in fact, is difficult to determine under filed conditions. So, we simply assume the value 0.04 in this study. Thus we can arrive at the following relations:

$$V_{0c} = (5.3 \sim 7.3) \cdot \sqrt{d} \cdot h^{1/6} \tag{7}$$

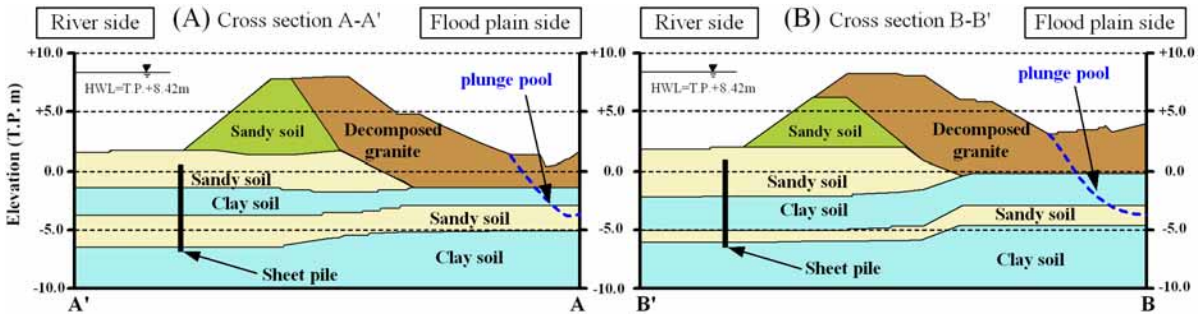

Fig. 14 Soil strata in cross sections A-A' and B-B' through the levee (adapted from Toyooka office, 2005b).

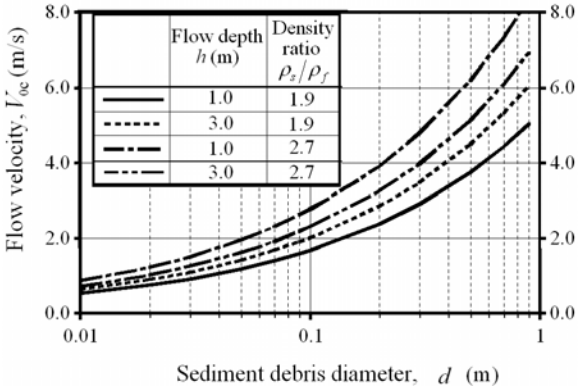

Fig. 15 Relations between critical flow velocity and sediment debris diameter

The relations between the critical flow velocity, V_{0c}, and particle diameter, *d*, are shown in Fig. 15 for four sets of flow depth *h* and density ratio ρ_s/ρ_f.

We suppose that the maximum size of the sediment debris occurring in the flood plain was 50cm or so, as realized by the clay lumps. Note herein that the levee construction was essentially with decomposed granite soil. The grain sizes involved may not exceed 30cm. If the sediment debris is 50cm in diameter, then we can read off from Fig. 15 a range of the critical velocities $V_{0c} = 3.8 \sim 4.5$ m/s for the density ratio equal to 1.9. This estimation should be applicable to the inundating water that flew down the paddy field beyond the plunge pool. A view of such an area after the event is presented in Photo. 4. Many clay lumps can be seen left on the severely eroded surface of the clayey subsoil. The surface conditions were markedly different from the adjacent zone where the rice roots remained. It will thus be worth exploring the stream power that can completely erode such rice roots.

6. Discussion

This section concisely discusses future directions along which digital geomorphological representation may advance for purposes of reducing risks of inundation disasters in flood-prone river basins.

One of the important considerations is to share the GSI's high-resolution spatial data framework designated Digital Map 2500. An example is shown in Fig. 16. This representation was made possible by superimposing the digital topographical dataset obtained from the photo-theodolite survey on a Digital Map 2500 of KINKI-1. The accuracy of our photo-theodolite surveying may be confirmed in Fig. 16 by referring to the locations of stable structures, such as building-2 which has fortunately stood essentially intact.

Another important consideration is to make best use of geographical classification maps that were designed to

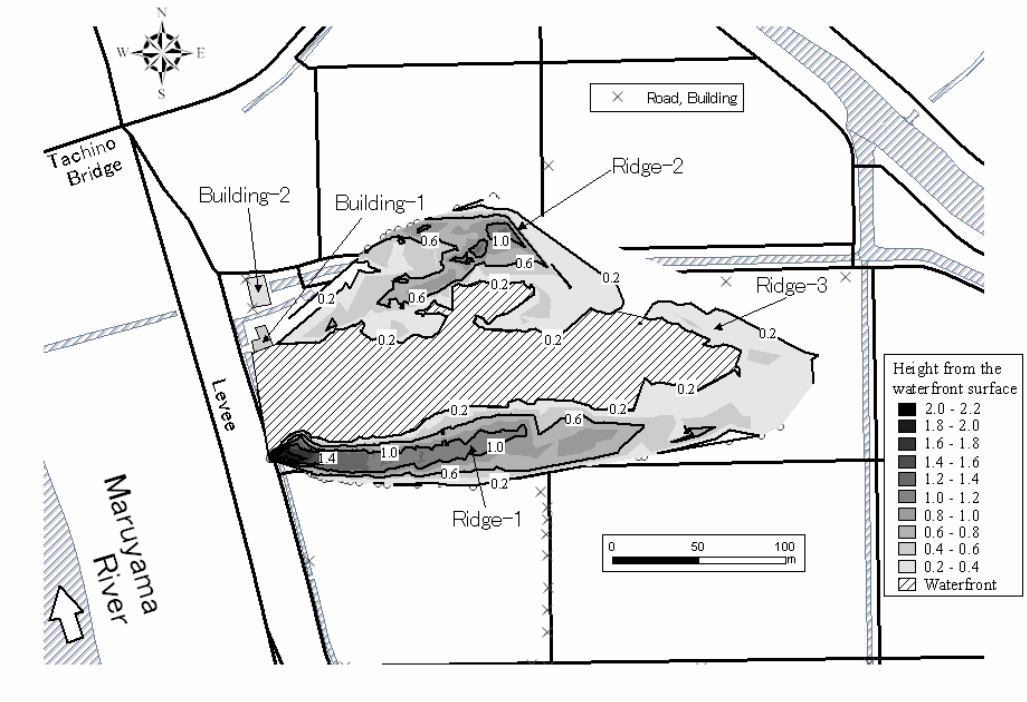

Fig. 16 Contours of topographical changes that are overlain onto a digital numerical map available from GSI

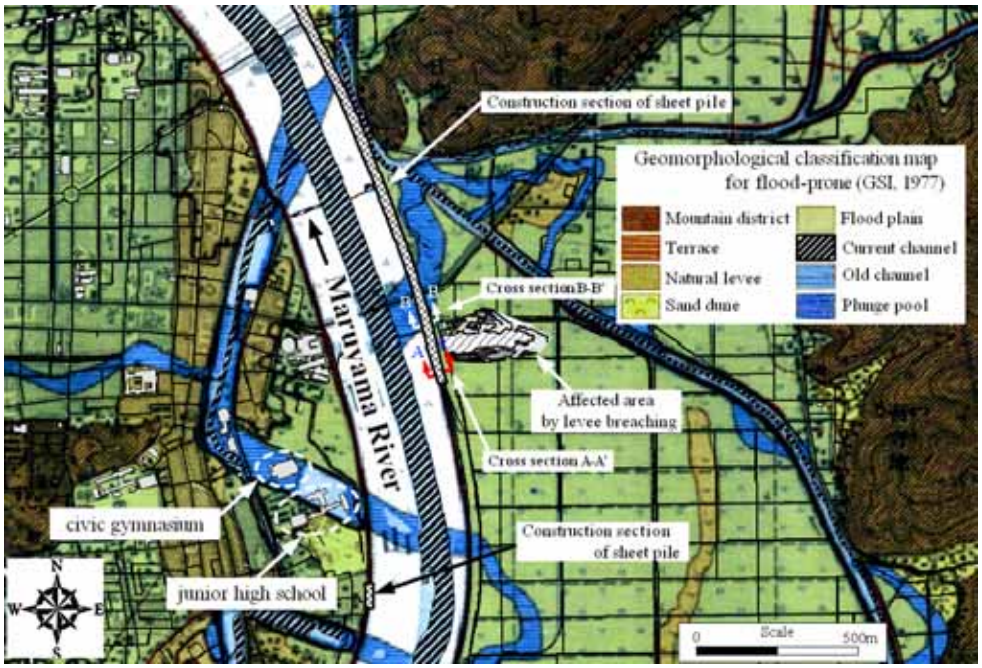

Fig. 17 Digital topographical data set superimposed on a digital image of the GSI-issued

record a range of flood-related morphological features, such as plunge pools, old channels, natural levees and sand dunes. Such a GSI-issued classification map is available for the Maruyama River basin and is represented in Fig. 17. Note herein that the classification map was initially published in 1977 and has recently been reprinted without any updating. Accordingly, it is informative and useful in its present form, but calls for special care regarding the land-use evolution that has occurred over the past thirty years or so. For instance, one may notice a few buildings standing on a part of the old meandering course of the Maruyama River. The shift in the river course was performed by the authority concerned as part of the extensive river training work. So, we believe that the old-channel site should have turned into land with well engineered designs.

The purpose of plotting the 2004 crevasse-splay sedimentary features on the 1977 map was to draw attention to the extent of the levee-breaching case which we surveyed using the digital photogrammetry. It really was a record-worthy large event.

As far as the management of flood-related hazards is concerned, the representation of old channels or the like on a geomorphological classification map is just a start for thorough engineering assessment. Indeed, a range of important engineering measures should be represented as well, as illustrated in Fig. 17. Note, for instance, a long stretch of sheet piling on the right bank of the Maruyama River. The sheet piling was performed many years ago so as to reinforce the seepage-vulnerable areas. Accordingly, we think that the location of the well treated old channel near Tachino should not directly affect the 2004 levee-breaching case. This statement may be supported by the observation that the foundation soil below the levee withstood the October 2004 excessively high flood stage.

7. Conclusions

The sedimentary features induced by the levee breaching have been discussed based on the digital photogrammetry survey as well as on the available technical information (Toyooka Office, 2005a). The digital topographical dataset was extensively analyzed using GIS. The principal conclusions drawn are as follows:

1) The digital photo-theodolite survey proved to be an effective methodology for obtaining a set of high-resolution topographical data within a relatively short time span.
2) The configurations of ridges 1 and 2 were precisely evaluated, revealing that they accounted for a large part of the sediment yield due to the levee breaching.
3) The presence of the competent clayey subsoil in the flood plain gave a physical constraint to the extent

of the plunge pool formed. Also, it led to the production of many clay lumps that were finally left on the flood plain beyond the plunge pool.

4) A bedload transport analysis by taking note of the size of the clay lumps yielded an upper-bound to the velocity of the inundating water, namely 4 m/s or thereabouts.

5) The digital topographical dataset obtained from the photo-theodolite survey is of high resolution and can readily make a GIS database.

6) The print-version of geographical classification maps for flood-prone areas is informative in its own right, but requires updating in a digital format to allow for land-use evolution as well as a range of relevant engineering measures. This is demonstrated in the discussion of Fig. 17.

Acknowledgements

The authors' special thanks go to the Toyooka Office, MLIT for the helpful technical discussion. Professor Yuichiro Fujita kindly made a photograph (Photo. 2) available to the authors. The assistance of Mr. Shinichi Akamatsu, Dr. Amiruddin and Mr. Kenzo Suyama in the data processing regarding the photo-theodolite survey would be greatly appreciated.

References

Azuma, R., Sekiguchi, H., Amiruddin and Ono, T. (2005): Levee breaching and associated sedimentary features on adjacent paddy field, Proc. of International Symposium on Fluvial and Coastal Disasters, Kyoto (on CD-ROM).

Geographical Survey Institute (1977): Geomorphological survey map for flood control of Toyooka.

Geographical Survey Institute (2005): Digital Map (Spatial Data Framework), KINKI-1.

Iwagaki, Y. (1956): Fundamental study on critical tractive force, Journals of JSCE, Vol.41, pp.1-21.

Ono, T. and Hattori, S. (2002): Fundamental principles of image orientation using orthogonal projection model, remote sensing and spatial information sciences, Vol.34, No.B3, pp.194-199.

Ono, T., Akamatsu, S. and Hattori, S. (2004): A long range photogrammetric method with orthogonal projection model, Int. Archives of Photogrammetry and Remote Sensing and Spatial Information Sciences, Vol.35, No.B3/1, pp.1010-1015.

Oya, M., Maruyama, Y., Umitsu, M., Haruyama, S., Hirai, Y., Kumaki, Y., Nagasawa, R., Sugiura, M., Kubo, J. and Iwahashi, J. (1998): Guidance for reading and making the geomorphologic classification map, Kokon shoin Publishers, Tokyo(in Japanese).

Toyooka River and National Highway Office/Kinki Regional Development Department/Ministry of Land, Infrastructure and Transport (2005a): Report of investigation committee of Maruyama-river levee (in Japanese).

Toyooka River and National Highway Office/Kinki Regional Development Department/Ministry of Land, Infrastructure and Transport (2005b): 1st conference material of investigation committee of Maruyama-river levee (in Japanese).

Uda, T., Mochizuki, T., Fujita, K., Hirabayashi, K., Sasaki, K., Hattori, A., Fujii, M., Fukaya, A. and Hiradate, O. (1997): Hydraulic stability and erodibility of rich-in-nature-type bank protection works, cohesive soil and short vegetation, Documents of Public works Research Institute, 3489(in Japanese)

超過外力に対する河川堤防の耐水性能評価と流域減災システムへの適用に関する研究

東良慶・関口秀雄・小野徹*

*京都大学 工学研究科 都市環境工学専攻

要旨

近年，都市化の進展と気象水文現象の極値の増大傾向が相乗し，洪水氾濫災害が顕在化している．これらは現行の堤防による治水システムが持つ根本的な課題を浮き彫りにさせており，超過洪水による沿川地域の被災レベルを極力軽減する方策の開発が求められている．本研究では，デジタル写真測量解析により2004年円山川堤防破堤にともなう堤内地の微地形変化の計測および堆積物移動収支の評価を行った．さらに，計測結果をGISデータベース化し，デジタル化した治水地形分類図と結合することにより，デジタル治水地形環境評価の手法を示した．

キーワード:破堤，河川堤防，微地形計測，治水地形分類図